

Computational methods for the analysis of, non-contact creep deformation, in ZrB₂–SiC composites

Xiao Ye, Robert W. Hyers*

Department of Mechanical and Industrial Engineering, University of Massachusetts, 160 Governors Dr., Amherst, MA 01003, USA

Available online 7 May 2010

Abstract

A need for higher service temperatures is driving development of new, higher temperature materials that are resistant to creep. However, conventional methods of measuring creep become increasingly difficult over about 1700 °C. A non-contact method with the capability of measurements at much higher temperature has been demonstrated on niobium using centrifugal loading of a spherical sample. Recent efforts have been made to extend this method to lower temperatures and higher stresses. Using material properties from the literature, we performed finite element simulations to determine the range of experimental parameters over which non-contact measurements of creep can be readily finished within a reasonable time duration for ZrB₂ and ZrB₂ + 25 vol.% SiC. Results from finite element analysis (FEA) model shows that the experiments are feasible at an angular velocity of 32,000 rps and a temperature 1900 °C for ZrB₂ + 25 vol.% SiC, but not for the pure ZrB₂ under the range of experimental conditions available.

© 2010 Elsevier Ltd. All rights reserved.

Keywords: Creep; Borides; Composites; Ultra-high temperature ceramics

1. Introduction

Modern applications such as rocket nozzles, leading edges of hypersonic airplanes, and next generation turbine blades place demanding requirements on ultra-high temperature ceramics. Besides requirements for the general mechanical strength and oxidation resistance, at high temperature, creep resistance is one of the most crucial criteria. UHTCs, including transition metal carbides, oxides and borides are of current interest for these applications. Zirconium diboride (ZrB₂) is characterized by a high melting point (3040 °C), high hardness (22 GPa) and good corrosion resistance due to its high percentage of covalent bonding.¹ However, at temperature greater than 650 °C, its resistance to chemical attack by oxidation is not satisfactory to accommodate atmospheric applications. In order to improve its oxidation resistance at elevated temperature, different additions have been introduced. Among them, 25 vol.% SiC (silicon carbide) is currently the most promising for applications in oxidizing environments.²

1.1. Fundamental creep behavior

Creep is defined as a time-dependent deformation under constant load that usually should be included into consideration when a material is subjected to a temperature higher than half of its absolute melting point and a stress lower than its yielding stress. The rate of creep is affected by various factors, such as material properties, temperature, and applied stress. Despite the differences among various creep mechanisms, creep behavior generally can be divided into three stages based on their different creep rate characteristics. In stage 1 (transient creep), the creep rate decreases until a minimum steady state is reached, which is stage 2. Examination by transmission microscopy examination shows that at the beginning stage material structure evolves with a significant accumulation of strain, which corresponds to a dramatic rise in dislocation density. And then during the following stage 2, speed of new dislocation generation and annihilation among dislocation balance to each other to reach a steady state macroscopically. In stage 3, creep rate rises again until fracture.

1.2. Experimentally determined creep behavior in UHTCs

Talmy et al.³ characterized flexural creep of ZrB₂ + 0–50 vol.% SiC as a function of temperature

* Corresponding author. Tel.: +1 413 545 2253; fax: +1 413 545 1027.
E-mail address: hyers@ecs.umass.edu (R.W. Hyers).

(1200–1500 °C), tensile stress (30–180 MPa) and SiC particle size (2 and 10 μm) in ambient air via four-point flexural creep test. In this geometry, the stress state within the gauge length is a single extensional stress, varying linearly from the maximum tension at one face of the sample to maximum compression at the other face. Therefore, the von Mises stress is equal to this extensional stress, as all other components are zero.

The creep rate increased with increasing SiC content, temperature, stress, and with decreasing SiC particle size, especially at temperatures above 1300 °C. The activation energy of creep turned out to be a function of SiC content and increased linearly with it for ceramics containing 0–50 vol.% 2 μm SiC. At 1400 °C, the reported stress exponent was 1.1 for pure ZrB₂ and 0.7 for ZrB₂ + 25 vol.% 2 μm SiC, which indicated for both compositions diffusional creep had a great contribution to total creep deformation. Their data indicate that the stress exponent n increases with temperature for the composite with 50% SiC, indicating a change in mechanism around 1400–1500 °C. However, there are not enough data reported to determine whether or not such a change in mechanism occurs, or at what temperature, for the compositions of interest in our study. The data we used from their paper is summarized in Table 1.

The thermal activation energy depends mainly on material's composition. The activation energy for creep is the same for Nabarro–Herring creep and power law creep, as both are limited by the diffusion of vacancies through the bulk. The activation energies derived from Talmy's experiment are 130 kJ/mol for pure ZrB₂ and 276 kJ/mol for ZrB₂ + 25 vol.% SiC.³

Melendez-Martinez et al.⁴ evaluated creep behavior of pure ZrB₂ and ZrB₂ + 4 wt.% Ni at temperatures between 1400 and 1600 °C and at stresses ranging from 47.0 to 472.3 MPa for pure ZrB₂ and 10 to 63.5 MPa for Ni-doped ZrB₂. The compressive creep test was performed in controlled argon atmosphere via a prototype dead-weight load device on specimens. The following mechanical properties were measured: elastic modulus (E), flexural strength (S), microhardness (H_v 1.0). Pure ZrB₂ showed only little creep deformation at temperature below 1400 °C and stress below 298 MPa. The reported stress exponent was 1.7 at 1500 °C and 0.6 at 1600 °C below 220 MPa. The Ni-doped ZrB₂ failed catastrophically for stress high than 25 MPa and shows a ductile behavior only at lower stress. The stress exponent was 1.5 at 1500 °C and stress was between 10 and 20 MPa. This behavior may be attributed to the presence of Ni-rich grain boundary phases at triple points of the grain structure.

1.3. Non-contact measurement of creep behavior

Since creep resistance is an important criterion in demanding applications, accurate measurement of creep behavior of candidate materials will be required. At high temperature, materials are highly reactive. Reaction with the test fixtures generally excludes conventional method for measuring creep above about 1700 °C. A group in UMASS has been working on non-contact measurement of creep behavior since 2004. Lee et al.⁵ used Electrostatic Levitation (ESL) to levitate spherical Nb specimen under high vacuum ($\approx 10^{-7}$ Torr) at NASA Marshall Space Flight Center (MSFC) in Huntsville, AL. This apparatus has a

Table 1

The experimental parameters from selected experiments by Talmy et al.³.

Material composition	von Mises stress (MPa)	Stress exponent	Activation energy (kJ/mol)
ZrB ₂	100	1.1	130
ZrB ₂ + 25 vol.% SiC ^a	100	0.7	276

^a Particle size of SiC is 2 μm .

demonstrated capability to process samples at extremely high temperatures, having been used to melt tungsten (3410 °C).⁶

Specimens were stabilized via three pairs of orthogonal electrodes controlled by PID control-loop. A 200 W YAG laser beam was cast on the sphere to heat and rotate the sample at many thousands of revs/s, resulting in sufficient load to cause sample to creep. The shape of the spherical sample was captured with high speed digital camera and the captured images were analyzed to determine the creep ratio (strain in rotating axis divided by strain in equatorial plane) of the sample. Meanwhile an ANSYS model was established to simulate creep behavior of the spherical model and predict the creep ratio at different stress exponents. By comparing the experimental creep ratio to the creep ratio curve generated with FEA predicted data and interpolation, the stress exponent of the sample can be determined, which further helps to determine the creep mechanism. The stress exponent measured in this way agrees with conventional tensile measurement.

2. Procedure

In this paper, an ANSYS model of a spherical sample was built to simulate creep behavior of monolithic ZrB₂ and ZrB₂ + 25 vol.% SiC. Inputs of this model include sample size, angular velocity of the rotation, temperature, density, Young's modulus, Poisson's ratio, activation energy, creep stress–strain rate relationship. These inputs were collected from the available literature and extrapolated to conditions where previous measurements are not available. The outputs of the model include the deformed shape of the model at arbitrary time and the distribution of the stress and strain on and inside of the deformed sphere. The simulation results will help to evaluate the feasibility of using this technique for UHTC's and to plan the experimental matrix.

2.1. Mechanical properties

Recently, ZrB₂ and ZrB₂-based composites have been densified by various methods, including hot pressing, reactive hot pressing, plasma sintering and pressureless sintering. Slight changes in processing conditions, such as temperature, thermal history, hold time, pressure, or species and quantities of additives will all have reflections in product's mechanical properties.

The reported material properties for densified ZrB₂ and ZrB₂ ceramics containing 10, 20 and 30 vol.% SiC particulates at room temperature were taken from Chamberlain et al.⁷ Corresponding properties for ZrB₂ + 25 vol.% SiC at room temperature were interpolated by taking arithmetic mean of materials with close

Table 2

Basic material properties (density, Young's modulus and Poisson's ratio) for pure ZrB₂ and ZrB₂ + 25 vol.% SiC used in the ANSYS model.

Material	Density (g/cm ³)	Young's modulus (GPa)	Poisson's ratio
Pure ZrB ₂	6.26	489	0.15
ZrB ₂ + 25 vol.% SiC	5.58 ^a	475 ^a	0.15

^a Interpolated data.

composition, giving 5.58 g/cm³ for density and 475 GPa for Young's modulus.

At elevated temperature, it is reasonable to assume that the density was still approximately the same as at room temperature. However, Young's modulus would experience a drastic drop. It was reported that other refractory composites, such as HfB₂, HfC_{0.98}, HfC_{0.67}, and HfN_{0.92}, would experience a modulus loss as much as 75% at high temperature.² Accordingly, in order to account for this modulus loss, a Young's modulus of 120 GPa was used for pure ZrB₂ and 130 GPa for ZrB₂ + 25 vol.% SiC for temperatures considered in our simulation.

Another mechanical property required for ANSYS model is Poisson's ratio. In contrast to other properties, it is insensitive to additives as well as to porosity caused by different processing conditions. It remains almost constant (approximately 0.15) for ZrB₂–MoSi₂–SiC composites with varying compositions.^{8–10} Based on this, Poisson's ratio was taken as 0.15 for both pure ZrB₂ and ZrB₂ + 25 vol.% SiC in our simulations.

The material properties for both materials used in the simulations are listed in Table 2. Though there could be some deviation from the real value of these properties in Talmy's experiment, these approximation would have a considerable impact on only the elastic deformation, which is trivial compared to the creep deformation (plastic deformation) of the specimen sphere. Therefore, the accuracy of these estimates should be sufficient for the present study.

2.2. Finite element analysis

2.2.1. Determination of creep mechanism and model parameters

The purpose of our simulation is to propose reasonable range of experimental parameters for research of creep behavior of ZrB₂ and ZrB₂ + 25 vol.% SiC within time duration at an order of several hours.

Previous work by our group³ using this technique used Nb samples deformed to 9% equatorial strain in 1–4 h, corresponding to a strain rate of $2 \times 10^{-5} \text{ s}^{-1} \sim 8 \times 10^{-5} \text{ s}^{-1}$. Accordingly, 10% equatorial deformation was taken as the target for the proposed experiments, and the model was used to determine the

Table 3

Input parameters of Norton creep model for ZrB₂ and ZrB₂ + 25 vol.% SiC as well as estimated creep rate.

Material	Coefficient (s ⁻¹)	Angular velocity (rps)	Temperature (°C)	Estimated creep rate (s ⁻¹)
Pure ZrB ₂	3.96×10^{-13}	32,000	2000	$3.2 \times 10^{-7} \text{ s}^{-1}$
ZrB ₂ + 25 vol.% SiC	2.09×10^{-4}	32,000	1900	2.05×10^{-5}

The estimated creep rate for the pure ZrB₂ is two orders of magnitude below the targeted range, while the rate for the composite is within the targeted range.

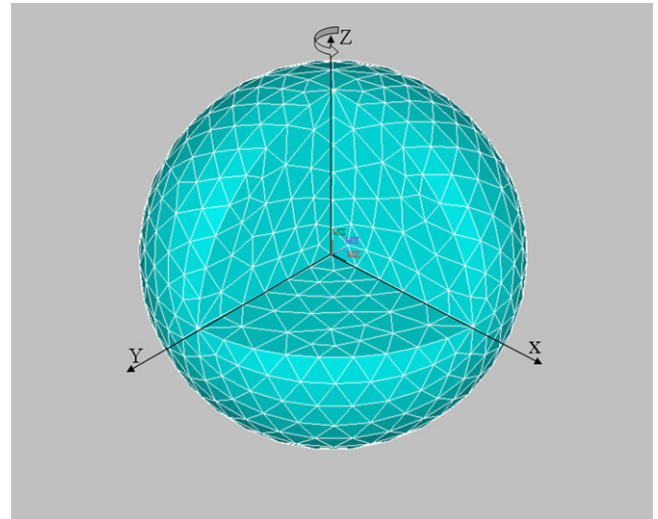


Fig. 1. Spherical model meshed with 10-node tetrahedral SOLID 186 elements: a quarter of the upper hemisphere was removed to show the mesh inside of the sphere.

experimental conditions that should be chosen to give a similar strain rate, $\sim 10^{-5}/\text{s}$.

Of the 13 featured implicit creep models of simulating primary and secondary creep behavior, the Norton model (Eq. (1)) was chosen for these simulations not only for its ability to model power law creep, but also its programming-friendly representation.

$$\dot{\epsilon} = C\sigma^n e^{\left(-\frac{Q}{RT}\right)} \quad (1)$$

where $\dot{\epsilon}$ is the strain rate, coefficient C is a material constant, σ is the von Mises stress for multiaxial loading, n is the stress exponent, Q is the activation energy, and R is the universal gas constant, which equals 8.314 J/mol K.¹¹

All input parameters of the FEA model are given in Table 3.

2.2.2. FEA model

A 3D rotating sphere sample model was built in ANSYS. SOLID 186 element was chosen based on the descriptions of ANSYS User's Manual. It was designed for simulating plasticity, hyperelasticity, creep, stress stiffening, large deflection and large strain. Fig. 1 shows the grid used for these computations. Tetrahedral elements suitable for an irregular and deforming mesh are employed. A uniform grid size 0.0002 mm was used to mesh the spherical model, which results in 5199 elements and 7891 nodes. Nodes in X–Y plane were constrained in Z direction and nodes on Z axis was constrained in both X and Y directions. Consequently, the node in the center of the sphere was constrained in all three directions.

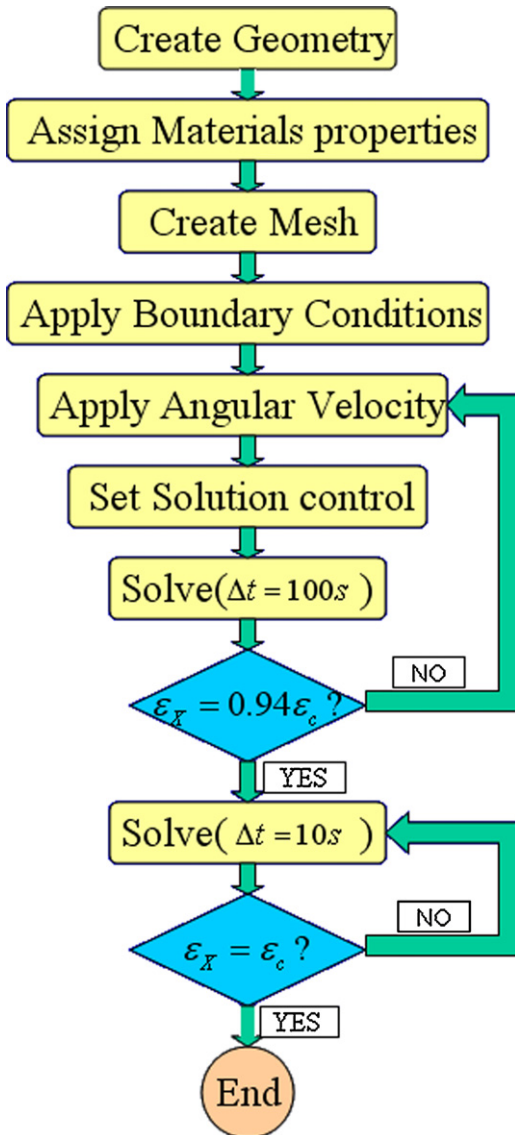


Fig. 2. Flowchart of the ANSYS analysis scheme. ε_x is the equatorial horizontal displacement and $\varepsilon_{\text{final}}$ stands for the 10% horizontal strain stop criterion.

The centripetal load was applied in the model by constant angular velocity. During ANSYS solving process, different time steps were used to optimize simulation time, with larger time steps in the early stages when the deformation rate is small, and smaller steps later as the stop condition is approached. The flow chart below (Fig. 2) depicts current finite element analysis scheme.

3. Results and discussion

3.1. Analytical results

The maximum shear stress in the center of the spherical sample can be analytically evaluated by the following equation:

$$\tau = 0.211 \omega^2 r^2 \rho \quad (2)$$

where ω is the angular velocity (rad/s), r is the radius of the sphere, ρ is the material density.¹² In the simulation, considering the current capability of the ESL apparatus, angular velocity of the FEA model was taken as 201,060 rad/s (32,000 rps). So, the shear stress in the center of the sphere should be close to 65 MPa for pure ZrB₂ and 58 MPa for ZrB₂ + 25 vol.% SiC. The geometry of the sample and its loading determine the intrinsic proportional relationship between von Mises stress and the shear stress: the von Mises stress at the center of the sphere is 1.88 times the shear stress there. Hence, the von Mises stress in the center of the sphere can be roughly estimated to be 122 MPa for pure ZrB₂ and 109 MPa for the composite at 32,000 rps, which was taken as the upper limit of the feasible range for the current apparatus.

The stress exponent is determined by the creep mechanism, which is itself dependent on temperature. For diffusional creep usually dominant at low stress, such as Coble creep and Nabarro–Herring creep, n is close to 1, while for power law creep, which usually happens at high stress, n is greater than 1. Referring to Table 1, the reported stress exponent for pure ZrB₂ is 0.7 and 1.1 for ZrB₂ + 25 vol.% SiC. At 1400 °C and 100 MPa von Mises stress³ and the strain rates are only $2.1 \times 10^{-8} \text{ s}^{-1}$ and $2.2 \times 10^{-7} \text{ s}^{-1}$, respectively. In order to raise the strain rate to shorten experiment time, the only practical means left is to raise temperature. If the dominant creep mechanism (diffusional creep) did not change at higher temperature, the stress exponent would still be 0.7 and 1.1 for pure ZrB₂ and the composite, respectively. It is found that there is no practical temperature for pure ZrB₂ to reach $\sim 10^{-5} \text{ s}^{-1}$ strain rate at this stress. To reach the desired creep rate at 2000 °C, for example, a von Mises stress of about 2800 MPa is predicted, corresponding to a rotation rate of over 150,000 rps. At 32,000 rps and 2000 °C, the predicted creep rate is only $3.2 \times 10^{-7} \text{ s}^{-1}$, corresponding to an experiment duration of about 100 h to reach 10% strain.

For the composite, a temperature as high as 1900 °C would be necessitated to decrease the experiment time to within 4 h at a rotation rate of 32,000 rps.

3.2. Numerical results

The equatorial radius after an elapsed time of 11,972 s (~ 3.3 h) was predicted to be $1.21 \times 10^{-3} \text{ m}$ with FEA analysis, which corresponded to the stop criterion of 10% horizontal strain. The time history plot of equatorial displacement in X direction was shown in Fig. 3. The constant strain rate, which is the slope of the curve, is consistent with the characteristic of secondary creep simulated. Also, dependence of horizontal displacement on radial position was plotted in Fig. 4. The horizontal displacement contour in XZ cross-section was plotted in Fig. 5. The von Mises stress dependence on radial position at the end of the simulation was plotted in Figs. 6 and 7 and in 2D and 3D, respectively. The von Mises stress at the center of the sphere is 108 MPa, which is very close to the previous estimate. The stress profile agrees well with analytically predicted stress profile.⁵

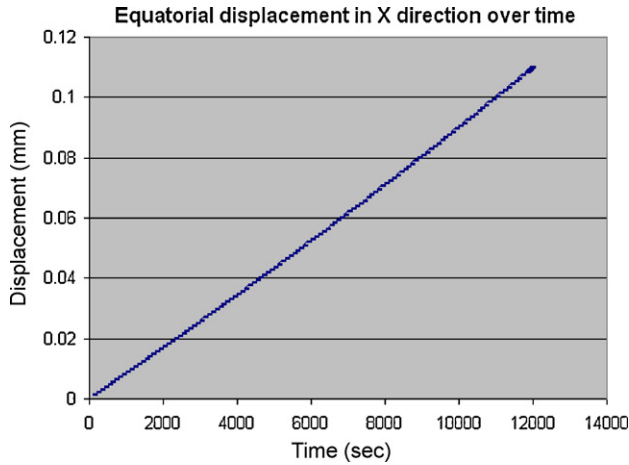


Fig. 3. Time history plot of equatorial displacement in X direction of ZrB₂ + 25 vol.% SiC at 32,000 rps and 1900 °C. The slope of the curve is almost constant, which is consistent with the characteristic of the secondary creep simulated in the mode.

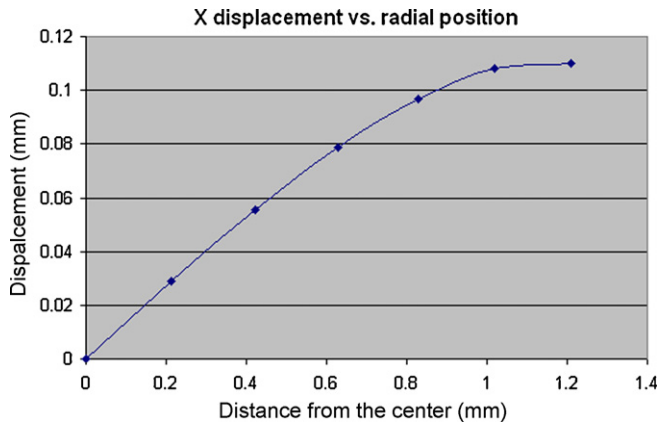


Fig. 4. Dependence of horizontal displacement on radial position in equatorial plane of ZrB₂ + 25 vol.% SiC at 32,000 rps and 1900 °C.

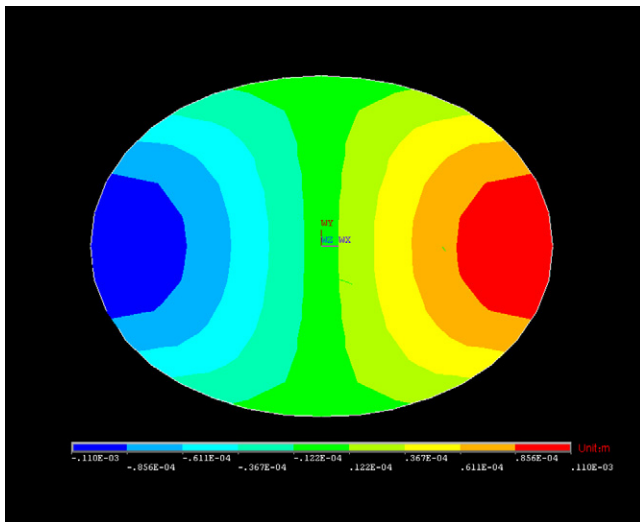


Fig. 5. Horizontal displacement contour of the XZ plane of ZrB₂ + 25 vol.% SiC at 32,000 rps and 1900 °C.

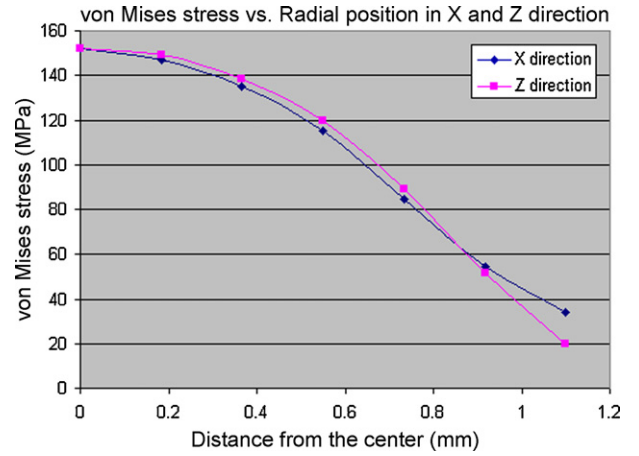


Fig. 6. von Mises stress plot of ZrB₂ + 25 vol.% SiC deformed at 32,000 rps and 1900 °C.

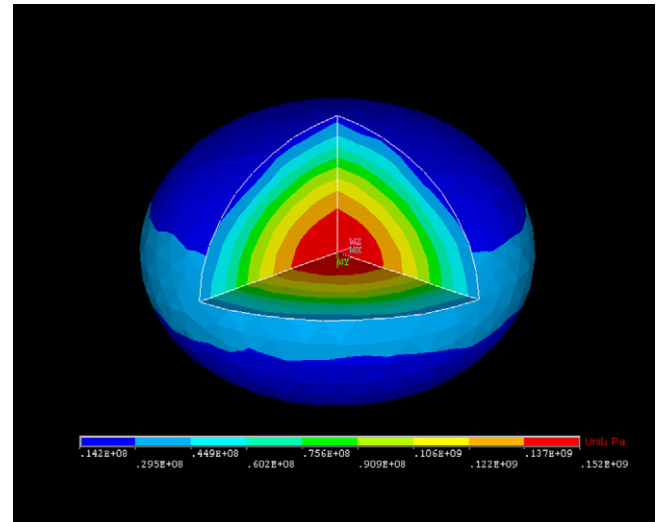


Fig. 7. von Mises stress contour of ZrB₂ + 25 vol.% SiC deformed at 32,000 rps and 1900 °C. A quarter of the upper hemisphere was removed to show the mesh inside of the sphere.

3.3. Sensitivity analysis

For a particular material, two independent variables, temperature and angular velocity (von Mises stress), determine the creep strain rate, which further determines the experiment duration.

For a temperature change ΔT small enough not to change the creep mechanism, so that the stress exponent n and leading coefficient C are consequently not changed, then according to Eq. (1):

$$\frac{\dot{\epsilon}_2}{\dot{\epsilon}_1} = \frac{C\sigma^n \exp\left(\frac{Q}{R(T+\Delta T)}\right)}{C\sigma^n \exp\left(\frac{Q}{RT}\right)} = \exp\left(\frac{Q}{R} \frac{\Delta T}{T(T+\Delta T)}\right) \quad (3)$$

where $\dot{\epsilon}_1$ and $\dot{\epsilon}_2$ denote the strain rate before and after the temperature change, respectively. For pure ZrB₂ at 2000 °C, the strain rate doubles after a temperature rise of 254 °C, while for ZrB₂ + 25 vol.% SiC at 1800 °C, the strain rate doubles after a temperature rise of 93.8 °C at a given rotation rate.

The von Mises stress is a function of both strain (shape of the sphere) and angular velocity. However, at a given strain, the relationship between the von Mises stress and the shear stress is fixed at every point in the sample. Furthermore, the shear stress is proportional to the square of the rotation rate, so the von Mises stress must be also. So, the change in strain rate due to a change $\Delta\omega$ in rotation rate is:

$$\frac{\dot{\epsilon}_2}{\dot{\epsilon}_1} = \left(\frac{\omega + \Delta\omega}{\omega} \right)^{2n} \quad (4)$$

For $\text{ZrB}_2 + 25 \text{ vol.}\% \text{ SiC}$, if the initial angular velocity is 201,060 rad/s (32,000 rps), 10% increase in strain rate would require a 14,164 rad/s (2254 rps) or 7% increase in angular velocity at a given temperature. For the pure ZrB_2 , the same 10% increase in strain rate would require a 4.4% increase in rotation rate.

4. Summary and conclusions

A model of a creeping sphere was established in ANSYS. Rotating at an angular velocity of 201,060 rad/s (32,000 rps), the sphere was subjected to a maximum von Mises stress about 100 MPa at its center. The Norton model was used to depict this creep behavior. From the available literature, parameters in Norton model at 1400 °C were calculated for ZrB_2 and $\text{ZrB}_2 + 25 \text{ vol.}\% \text{ SiC}$, which functioned as a basis for extrapolation to nearby temperatures. In order to get a 10% equatorial deformation within several hours, the strain rate should be at the order of $10^{-5}/\text{s}$, which is comparable to our group's previous work.

The simulations show that such a fast creep rate is to be expected from the $\text{ZrB}_2 + 25 \text{ vol.}\% \text{ SiC}$ composite sample at 1900 °C and a very fast rotation rate of 32,000 revolutions per second. Although the method has been demonstrated only at speeds up to 11,000 rps, work is underway at UMASS and NASA to extend the experimental range to speeds over 30,000 rps.

For pure ZrB_2 , the results are less promising. The feasible load and temperature provide a strain rate only of the order 10^{-7} , which would require an experiment duration of about 100 h to reach 10% strain. Much higher rotation rates, approximately 150,000 rps, would be needed to achieve the target strain rate with this sample.

In conclusion, the model shows that the experiments are feasible for the 25% SiC composite, but not for the pure material,

with the current experimental limitations. With the extended range of rotational speed and stress, the range of applicability of the new method overlaps with conventional methods, while still providing the capability of measurements at much higher temperatures than conventional methods. Even higher stresses are needed to study very creep-resistant materials such as pure ZrB_2 .

Acknowledgement

The authors would like to acknowledge AFOSR (Dr. J. Fuller) for providing support for this project under STTR Phase I grant FA 9550-09-C-0089.

References

- Morz C. Annual mineral review zirconium diboride. *Am Ceram Soc Bull* 1995;**74**:165–6.
- Opeka M, Talmy IG, Wuchina EJ, Zaykoski JA, Causey SJ. Mechanical, thermal and oxidation properties of refractory hafnium and zirconium compounds. *J Eur Ceram Soc* 1999;**19**:2405–14.
- Talmy IG, Zaykoski JA, Martin CA. Flexural creep deformation of ZrB_2/SiC ceramics in oxidizing atmosphere. *J Am Ceram Soc* 2008;**91**(5):1441–7.
- Melendez-Martinez JJ, Dominguez-Rodriguez A, Monteverde F, Melandri C, de Portu G. Characterisation and high temperature mechanical properties of zirconium diboride-based materials. *J Eur Ceram Soc* 2002;**22**:2453–549.
- Lee J, Bradshaw RC, Hyers RW, Rogers JR, Rathz TJ, Wall JJ, Choo H, Liaw PK. Non-contact measurement of creep resistance of ultra-high-temperature materials. *Mater Sci Eng A: Struct Mater: Prop, Microstruct Process* 2007;**463**(1–2):185–96.
- Rogers JR, Hyers RW. Electrostatic levitation: an emerging materials characterization technique. In: *Presented at the TMS Annual Meeting*. 2008.
- Chamberlain AL, Fahrenholtz WG, Hilmas GE, Ellerby DT. High-strength zirconium diboride-based ceramics. *J Am Ceram Soc* 2004;**87**(6):1170–2.
- Guo SQ. Densification of ZrB_2 -based composites and their mechanical and physical properties: a review. *J Eur Ceram Soc* 2009;**29**:995–1011.
- Guo SQ, Nishimura T, Mizuguchi T, Kagawa Y. Mechanical properties of hot-pressed $\text{ZrB}_2\text{-MoSi}_2\text{-SiC}$ composites. *J Eur Ceram Soc* 2008;**28**(9):1891–8.
- Guo SQ, Kagawa Y, Nishimura T. Mechanical behavior of two-step hot-pressed ZrB_2 -based composites with ZrSi_2 . *J Eur Ceram Soc* 2009;**29**(4):787–94.
- Courtney T. *Mechanical behavior of materials*. Boston, MA: McGraw-Hill Co.; 2000, 293–347.
- Kiessig H, Essmann U. Flow stress of pure niobium between 2200 K and the melting point 2741 K. *Scripta Mater* 1985;**19**:989–92.